Title
MicroED in natural product and small molecule research

Journal
Natural Product Reports, 38(3)

ISSN
0265-0568

Authors
Danelius, Emma
Halaby, Steve
van der Donk, Wilfred A
et al.

Publication Date
2021-03-01

DOI
10.1039/d0np00035c

Peer reviewed

Published in final edited form as:

Nat Prod Rep. 2021 March 01; 38(3): 423–431. doi:10.1039/d0np00035c.

MicroED in natural product and small molecule research

Emma Danelius[a,†], **Steve Halaby**[a,b,†], **Wilfred A. van der Donk**[c], **Tamir Gonen**[a,b,d]

[a.]Department of Biological Chemistry, University of California Los Angeles, 615 Charles E Young Drive South, Los Angeles, CA90095

[b.]Howard Hughes Medical Institute, University of California Los Angeles, Los Angeles, CA90095

[c.]Department of Chemistry and Howard Hughes Medical Institute, University of Illinois at Urbana-Champaign, Urbana, IL 61801

[d.]Department of Physiology, University of California Los Angeles, 615 Charles E Young Drive South, Los Angeles, CA90095

Abstract

The electron cryo-microscopy (cryo-EM) method Microcrystal Electron Diffraction (MicroED) allows the collection of high-resolution structural data from vanishingly small crystals that appear like amorphous powders or very fine needles. Since its debut in 2013, data collection and analysis schemes have been fine-tuned, and there are currently close to 100 structures determined by MicroED. Although originally developed to study proteins, MicroED is also very powerful for smaller systems, with some recent and very promising examples from the field of natural products. Herein, we review what has been achieved so far and provide examples of natural product structures, as well as demonstrate the expected future impact of MicroED to the field of natural product and small molecule research.

Introduction

Natural products are important sources for drug discovery and continue to be the main inspiration for the development of new small-molecule drugs.[1] They display a broad structural diversity and a wide range of functions and biological activities. For example, FDA-approved natural product-based drugs for 2018 and 2019 include anti-cancer agents, antidepressants, anti-Parkinson, and anti-infectives.[1,2] Compared with traditional small molecules leads, natural products often have a more complex structure with higher molecular weights and more rotatable bonds and stereogenic centers, providing a higher potential to bind to and modulate the functions of difficult biological targets such as protein-protein interactions and transcription factors.[3,4] However, with these unique advantages also come challenges in structure elucidation.[5]

[†]These authors contributed equally.

Conflicts of interest

Patents filed 16/672,040; 63/013,874; 67/755,200

The methods most commonly used thus far for structural characterization of natural products are X-ray crystallography, mass spectrometry (MS) and nuclear magnetic resonance (NMR) spectroscopy, as well as computational prediction of NMR and other spectroscopic properties.[6–8] These methods have different benefits and are used in a complementary fashion. X-ray crystallography has been considered the gold standard for the structure elucidation of natural products, particularly as the absolute configuration can be established. However, the large amounts of material required for crystallization assays pose a serious challenge especially for natural products that are often obtained in vanishingly small amounts. A relatively new method that has shown great potential in the field of natural product research is the cryo-EM method MicroED.[9–11] In cryo-EM, frozen-hydrated samples are studied in a transmission electron microscope (TEM) at liquid nitrogen temperatures, either in imaging or diffraction mode, where the latter is used for MicroED. The method compares to X-ray crystallography in that samples are studied in the solid phase but it requires substantially less sample, and benefits from easier sample preparation, in some cases without the need for prior crystallization.[12–14] Also, MicroED can be used to derive the atomic structures of molecules directly from mixtures of several compounds,[12,14] which is not possible with other diffraction based methods.

MicroED theory and background

Electron diffraction dates back to the earliest days of electron microscopy, but due to several technical difficulties, electron diffraction was largely ignored for decades. The benefit of using electrons as compared to X-rays is that they interact more strongly with matter while depositing less energy into the crystal.[15] Despite being used successfully to solve structures with 2D crystals, the technique presented several challenges, such as low sensitivity of electron detectors, low signal-to-noise ratio, laborious data processing, and the limitation that only one image could be collected at a time.[16,17] An additional challenge posed for 3D crystals is dynamical scattering, that is when electrons undergo multiple scattering events instead of a single one leading to inaccurate spot intensities.

By comparison, the *resolution revolution* in cryo-EM, fuelled by the improvements in software and detectors, helped increase the availability of TEMs as researchers raced to solve structures of large proteins from single particles to resolutions that had not been possible before.[18] These efforts lead to the 2017 Nobel Prize in Chemistry.[19] At the same time, part of the *resolution revolution* in cryo-EM was the rebirth of electron diffraction as a technique to solve molecular structures from 3D nanocrystals known as MicroED.[9,10] Alongside with other non-cryogenic methods that were developed for hard materials,[20,21] MicroED was introduced into the field of structural biology in 2013. Following the first MicroED structure of lysozyme,[9] and the demonstration of continuous rotation MicroED,[22] today there are over 100 published protein structures in the protein data base (PDB) and many more in small molecule depositories. MicroED structures vary greatly and include soluble,[23,24] and membrane proteins,[25] protein-ligand complexes,[26–28] nanomaterials,[29,30] semiconductors,[31] natural products[11,32,33] and small molecules.[14,34–38] Importantly, many of these structures were previously unattainable by other methods.

The crystals used for MicroED data collection typically have a thickness in the nanometre range (Figure 1). Due to their small size, crystal identification using a conventional light microscope is often impractical. While drops with granular aggregates (Figure 1A) are of little use for X-ray crystallography they make promising targets for nanocrystals suitable for MicroED.[39] Unique to peptides, small molecules, and natural products, amorphous powders can also be used without any prior crystallization (Figure 1B). To confirm the presence of nanocrystals negative-stain EM can be used.[40] Upon treatment with a staining solution, the crystals will appear dark on a white background when viewed in the electron microscope (Figure 1C). Another method to identify crystals that are <1 μm is Second-Order Nonlinear Imaging of Chiral Crystals (SONICC), however, high symmetry crystals cannot be recognized.[41] Grids (Figure 2C) can also be screened for nanocrystals using the low magnification settings of the TEM (Figure 1D).[42]

One of the most critical steps in MicroED is grid preparation.[40] For small molecules and natural products, samples can be prepared at room temperature[12,13,43,44] or under cryogenic conditions.[45] When using the latter, the grids are plunged into liquid nitrogen, or liquid ethane to retain the frozen-hydrated state in vitreous ice. When amorphous powders (Figure 2A) are used for grid preparation, a homogenous powder is first obtained by placing a small amount of sample in between two coverslips and gently grinding it (Figure 2B).[14] The grids (Figure 2C) can then be placed on top of the powder or transferred to a tube along with the powder. After gently swirling the tube excess sample is removed and the grids are frozen and loaded into the cryo TEM.

Data collection for MicroED is performed using the TEM in diffraction mode while continuously rotating the sample (Figure 3A).[22] As opposed to discrete tilting of the sample, collecting movies of the diffraction (Figure 3B) by continuous rotation has the benefit of reduced dynamic scattering, faster data collection times, as well as a more accurate sampling of reciprocal space.[22] Importantly since the rotation mimics that of a crystal in rotation X-ray diffraction, software such as XDS,[46] iMosFlm[47,48] DIALS and ShelX[49] can be used to process the data and determine the molecular structure (Figure 3C).

Application to the field of small molecules and natural products

Crystallization is an art form and in reality, poorly understood. The process continues to be a trial-and-error effort that may take years before well-diffracting crystals are obtained.[39] Since natural products are typically flexible they tend to be difficult to crystallize. Also, the amounts of the natural product isolated from native sources is usually extremely small, and often large-scale crystallization is not feasible.[4] As the crystals used for MicroED are about a billionth of the size as compared to those used for X-ray diffraction, they are much more easily obtained, as demonstrated by the many novel and previously unattainable structures that have been reported by MicroED. For example, the first peptide structure determined by MicroED was the 1.4 Å resolution structure of the toxic core of α-synuclein which had resisted structural determination by X-ray for decades (Figure 4).[50] The structure was obtained using ‘invisible crystals’, i.e. crystals with dimensions smaller than the wavelength of visible light and thus invisible by optical microscopy. Remarkably, MicroED has also been used to rapidly derive atomic resolution structures directly from powders, i.e. without

the laborious and time-consuming crystallization assays.[12] Seemingly amorphous solids from silica gel chromatography and rotary evaporation or directly from a chemical supplier were used.[14] As described in the previous section, minute quantities were grounded and deposited on cryo-EM grids. Examples of this grid preparation include the analgesics acetaminophen[35] and orthocetamol,[51] the vitamins biotin[14,35] and niacin,[13] the alkaloid brucine,[14] the macrocyclic peptide thiostrepton,[14] the biosynthetic peptide VFA-thiaGlu,[11] and the directed evolution derivate of 3-methyloxindole, (*S*)-2-amino-3-((*S*)-3-methyl-2-oxoindolin-3-yl)propanoic acid (Figure 4).[32] Samples can also be evaporated out of ethanol directly onto grids.[44] Unlike any other structural biology technique, MicroED offers the possibility of determining atomic structures from compound mixtures. This approach was demonstrated using biotin, carbamazepine, cinchonine, and brucine, whose powders were mixed and deposited onto a single grid for MicroED. All four compounds could be identified from the same grid square and their structures were solved to atomic resolution (Figure 4).[14]

MicroED in drug discovery

Structure-based inhibitors of aggregation in amyloid formation.

Aggregated tau protein is linked to several neurological disorders, including Alzheimer's disease. The VQIINK segment of tau is the primary driver of the aggregation and formation of amyloid fibrils in the brain, and therefore inhibition of this segment may potentially halt the disease progression.[52] All efforts to grow crystals of this segment produces only nanocrystals, 10,000 times smaller than those previously used for structure determination of other tau aggregation segments. The 1.1 Å resolution structure of KVQIINKKLD solved by MicroED revealed the VQIINK-segment to form a face-to-face Type 1 homosteric zipper.[52] Based on this structure, a series of aggregation inhibitors were designed and shown to inhibit seeding by tau fibers with an activity in the low micromolar range, where the highest activity was obtained for tryptophan-containing peptidic inhibitors, making steric clashes and thereby preventing aggregation.[52] Similarly, structure-based inhibitors were developed for the Amyloid-β and human islet amyloid polypeptide (hIAPP) aggregate, which also form amyloid fibrils in Alzheimer's disease. Inhibitors based on the 1.5 Å MicroED structure of hIAPP were shown to reduce fibril formation at equimolar concentrations, and the inhibition was shown to be specific for the Amyloid-β – hIAPP target.[53]

Protein-Ligand interactions revealed by MicroED.

During HIV maturation, HIV-1 protease cleaves the Gag protein which triggers the assembly of mature, infectious particles. A potential therapeutic strategy is therefore blockage of the Gag – protease interaction. A known maturation inhibitor, bevirimat, based on a betulinic acid-like natural product, had been previously described to modulate this target with moderate efficiency[26]. Co-crystallization of the interacting fragment of HIV-1 Gag and bevirimat had proven unsuccessful for X-ray analysis. In contrast, the protein-ligand complex was determined from frozen-hydrated microcrystals by MicroED (Figure 5).[26]

The structure revealed both electrostatic and hydrophobic interactions providing the starting point for structure-based drug design and optimization for the development of more efficient maturation inhibitors.

Another more recent example of protein-ligand interactions determined by MicroED was that of the structure of a sulphonamide inhibitor bound to human carbonic anhydrase isoform II (HCA II). The 2.3 Å resolution complex revealed an active site zinc, as well as several electrostatic interactions consistent with previous X-ray structures.[27] Soaking small molecules into protein nanocrystals directly on the grid, was recently demonstrated.[28] The diffusion of small molecules into nanocrystals is extremely efficient leading to high occupancy and yielding excellent experimental density maps. These maps are critical for effective drug discovery and optimization. Furthermore, these findings suggest that MicroED may be a powerful technique for better understanding of the modes of action of natural products when crystallization with their targets has proven challenging.

Solving MicroED structures by different phasing methods

Peptide structure determination by MicroED using direct methods.

When X-ray diffraction is better than 1.2 Å resolution direct methods can be used to solve the molecular structures.[54] This approach was first demonstrated for MicroED data of four peptide segments from the amyloid core of the Sup35 prion protein.[55] This 685-residue yeast protein is often used as a model for its ability to form amyloid fibrils relevant for neurodegenerative diseases. In addition to demonstrating that dynamical scattering did not impede the structure determination, it was also shown that if the resolution is high enough, MicroED structures can be phased by direct methods. When compared to previously obtained structures using X-ray crystallography, a marked improvement in resolution was observed. For example, the peptide GNNQQNY was solved to 2.0 Å resolution using X-ray and 1.05 Å when using MicroED.[55] Since this proof-of-concept, other prion structures have been solved to sub-ångström resolution with hydrogens unambiguously assigned (Figure 6).[12] Other structures of peptides[45] and natural products[14] have also been solved from MicroED data using direct methods.

Peptide structure determination by MicroED using molecular replacement.

In cases where crystals diffract to a lower resolution, and a search model is available, molecular replacement can be used. For example, two new 11-residue segments of hIAPP were solved by MicroED using molecular replacement.[56] It is established that amyloid fibrils in type II diabetes are composed of hIAPP,[57,58] and as the full-length fibril has resisted crystallization, structures of several small segments have been successfully solved to determine the cause of the toxicity.[59,60] The crystals of such peptide segments longer than 7 amino acids usually do not diffract in X-ray.[50,56] On the other hand, the structures of the two 11-residue segments were determined to 1.9 Å (19–29 S20G) and 1.4 Å (15–25 WT) resolution by MicroED.[56] Existing programs used for X-ray crystallography were used for phasing, model building, and refinement. Two different approaches were used to phase the data. The S20G segment was phased from an idealized 7-residue poly-alanine while the WT peptide was phased using a model with a similar structure after dozens of different search

models were explored. The packing of the β-strands confirmed the toxicity in that the S20G segment was curved and had a sharp kink making it more stable and thereby more toxic, whereas the WT peptide was discovered to be a member of the recently discovered class of out-of-register segments with weak strand interactions.[61]

Experimental phasing of MicroED data using radiation damage.

An advantage of MicroED data collection is that the crystal is typically only exposed to a dose of ~0.01 e^{-} $Å^{-2}$ s^{-1},[10] which is orders of magnitude less than the dose for single-particle cryo-EM. However, the small crystals are still prone to damage caused by the high-energy electrons and similar to damage from X-rays, acidic side chains, disulfide bonds and metals are more susceptible.[45] Radiation damage can also be used to phase diffraction data. In the radiation damaged induced phasing (RIP) method, several data sets are collected for phasing from which differences in structure factors are calculated. The resulting maps are then used to compare the damage between the data sets.[62]

RIP was used to phase MicroED data from two data sets collected from the peptide GSNQNNF at a total dose of 0.17 $e^{-}Å^{-2}$ and 0.5 e^{-} $Å^{-2}$. The structures contained a zinc site that was identified from a Patterson difference map. From these maps initial phases were generated and used to model and refine the structure to 1.4 Å resolution, establishing RIP as an alternative method for MicroED molecular structure determination.

Determining absolute configuration by MicroED

As different stereoisomers might induce a different biological response, determining the absolute configuration of drugs and natural products is of great importance. As a case in point, the *S*-form of the drug thalidomide provided a calming effect for morning sickness in pregnant women, while the *R*-enantiomer caused birth defects.[63] Likewise, it is known that the *trans* isomer of the anti-cancer agent cisplatin is therapeutically inactive.[64] The majority of active pharmaceutical ingredients are chiral and their absolute configuration is typically determined by X-ray crystallography,[65] although NMR,[66] vibrational circular dichroism,[67] and X-ray powder diffraction,[21] have been used as well. While a recent report suggests that dynamical refinement could be used to determine the absolute configuration,[68] the utility of this approach is still to be tested.

Meanwhile, two other MicroED studies were successful in determining absolute stereochemistry by using internal standards.[11,32] In both cases one or more L-amino acids were attached to the molecule of interest and in this way, the stereochemistry of unknown centers was determined. In the first example, a ribosomally synthesized scaffold peptide with a nonribosomal modification and extension was studied.[11] Per previous studies on radiation damage,[45] this sulfur-containing peptide proved to be prone to radiation damage. Using a direct electron detector with high sensitivity and high frame rate the damage could be outrun and the structure of one of the isomers could be determined from femtograms of powder material to atomic resolution (Figure 7A). The structure revealed the modified amino acid to be of D-configuration, which in turn provided the stereochemical configuration of the natural product to be of L-configuration.[11] In the second example variants of tryptophan synthase, TrpB Pf_{quat} obtained by directed evolution were studied.

Some of these variants proved to have increased activity and were able to form a new quaternary stereocenter at the γ-position of its amino acid products by alkylation. The molecular structure and configurations of the γ-stereocenters of two of the products were determined via MicroED (Figure 7B).[32] These two studies emphasize the utility of MicroED to determine the stereochemistry of previously unknown natural products, biosynthetic intermediates, or enzymatic products.

Current limitations of MicroED for Small Molecules

As with any emerging technique, MicroED has several limitations and can benefit from continued development. One of the major obstacles in making this technique widely available is that instrumentation (e.g. cryo-electron microscopes and sample preparation equipment) as well as the required expertise are not yet readily available to laboratories worldwide. Even when the equipment is accessible, sample preparation and data collection strategies can vary so access to expertise is still important. Dedicated technology development centers, like the one recently established at UCLA called the MicroED Imaging Center, are necessary for further development and broadening the scope of the method and increasing the numbers of practitioners.

Another challenge posed by MicroED is the identification of microcrystals. As of now, there is no predominant technique and several of the methods explained above are used in combination. Lastly, determining absolute configurations of small molecules by MicroED has so far required the use of internal standards.

Impact of MicroED to the field of natural products

The potential impact of MicroED on natural product research is multifold. The most obvious application is structure elucidation of newly discovered compounds. The past decade has seen new approaches to natural product discovery that take advantage of the explosion in genomic information. Knowing the genetic capacity of an organism to produce specialized metabolites removes some of the uncertainty of traditional discovery methods and allows the use of comparative genomics for identification of biosynthetic gene clusters (BGCs) of interest.[69–75] To help prioritize which BGCs to study, powerful bioinformatics tools have been developed,[76] and to access new molecules encoded by these BGCs strategies have been devised for heterologous production by synthetic biology approaches[77–83] as well as complementary new methods to elicit production in native organisms.[72,84–87] Improved detection methods featuring mass spectrometry have also contributed to linking biosynthetic gene clusters to their products,[88–90] and have facilitated the discovery of new compounds. Finally, investigation of microorganisms from less traditional environments including microbiomes, endosymbionts, and unculturable organisms have provided novel sources of compounds. Collectively, these developments have led to much excitement that natural product discovery is entering a phase of rapid expansion. In principle, several of these approaches can be scaled in massively parallel fashion, thus potentially resulting in rapidly expanding numbers of new molecules. Two new bottlenecks would then loom: compound purification and structure elucidation.

NMR spectroscopy has been the method of choice to determine the structure of a new natural product.[91,92] For some select compound classes such as peptides, tandem MS can provide important information especially when used with molecular networking,[93] but this technique does not provide stereochemical information and also provides challenges for macrocyclic structures. NMR spectroscopy requires relatively high concentrations and hence good solubility, although cryo-probes and capillary methods have improved sensitivity and decreased sample volume for mass-limited samples.[94–98] Contemporary structure elucidation by NMR spectroscopy is relatively routine but can be time-consuming as multiple different pulse sequences are often required and interpretation can be challenging or non-definitive. Indeed, while not a major problem, incorrect structures of natural products have been reported in the literature.[5] Particularly difficult are the assignment of stereocenters that are far removed from other stereocenters.

As noted above, X-ray crystallography is powerful but requires large crystals, which in turn usually requires highly pure samples and relatively high quantities. Much excitement was generated in 2013 by the publication of a method that involved soaking solutions of compounds of interest with porous metal complexes that served as crystalline sponges.[99] Using this technology, a series of different non-crystalline guest molecules were structurally characterized by X-ray crystallography including the sesquiterpene guaiazulene and the plant natural product (−)-α-santonin. The authors also used the method to soak HPLC fractions with the porous metal frameworks in a method termed LC-single crystal crystallography. However, when they used the method to determine the stereochemistry of miyakosyne A, the assignment was later shown to be incorrect leading to questions about the utility of the method.[100] In subsequent years, the technology was optimized with respect to the crystalline sponge such that structures could be obtained faster and absolute configuration determined more reliably.[101–103] However, to date, the method has not been widely used for structure determination of newly discovered natural products.[104–106]

In this landscape of rapid expansion of new technology to produce novel natural products and the absence of truly rapid methods for structure determination, MicroED has the potential to help prevent structure elucidation from becoming a major bottleneck. The required equipment is becoming accessible to many laboratories, and as described herein, sample preparation is relatively simple. Although sample preparation methods and data acquisition still require optimization for individual compound classes, the technology has potential for high throughput structure elucidation and would be especially powerful if the structures of mixtures of unknowns can be determined.

Beyond its utility for natural product discovery, MicroED has logical applications in several other arenas important to the natural product community. The possibility to determine the stereochemical configuration of small amounts of advanced intermediates in total synthesis would facilitate streamlining such efforts. Similarly, structure determination of advanced intermediates in complicated biosynthetic pathways would help the elucidation of enzyme function and inform synthetic biology studies. And finally, the technique may prove powerful for the investigation of natural product mode of action. Widespread implementation of these additional applications would require the method to be accessible to non-specialists and a certain level of predictability of success. While certainly still facing

challenges, the coming years will undoubtedly see efforts to further develop MicroED into a mainstay tool for the natural product community.

Acknowledgments

The authors would like to thank all of the collaborators, national and international, who contributed over the years to the development of MicroED. We would also like to thank the following sources of funding: The National Institutes of Health P41GM136508 to T.G. and R01 GM 058822 to W.A.V.. The Gonen and van der Donk laboratories are supported by funds from the Howard Hughes Medical Institute. Wenner-Gren Foundations to E.D.

Notes and references

1. de la Torre BG and Albericio F, Molecules, 2020, 25, 745.
2. de la Torre BG and Albericio F, Molecules, 2019, 24, 809.
3. Harvey AL, Drug Discov. Today, 2008, 13, 894–901. [PubMed: 18691670]
4. Boufridi A and Quinn RJ, Annu. Rev. Pharmacol. Toxicol, 2018, 58, 451–470. [PubMed: 28968192]
5. Chhetri BKK, Lavoie S, Sweeney-Jones AMM and Kubanek J, Nat. Prod. Rep, 2018, 35, 514–531. [PubMed: 29623331]
6. Přichystal J, Schug KA, Lemr K, Novák J and Havlíček V, Anal. Chem, 2016, 88, 10338–10346. [PubMed: 27661090]
7. Lodewyk MW, Siebert MR and Tantillo DJ, Chem. Rev, 2012, 112, 1839–1862. [PubMed: 22091891]
8. Grauso L, Teta R, Esposito G, Menna M and Mangoni A, Nat. Prod. Rep, 2019, 36, 1005–1030. [PubMed: 31166350]
9. Shi D, Nannenga BL, Iadanza MG and Gonen T, Elife, 2013, 2, e01345. [PubMed: 24252878]
10. Nannenga BL and Gonen T, Nat. Methods, 2019, 16, 369–379. [PubMed: 31040436]
11. Ting CP, Funk MA, Halaby SL, Zhang Z, Gonen T and van der Donk WA, Science, 2019, 365, 280–284. [PubMed: 31320540]
12. Gallagher-Jones M, Glynn C, Boyer DRR, Martynowycz MWW, Hernandez E, Miao J, Te Zee CT, Novikova IVV, Goldschmidt L, McFarlane HTT, Helguera GFF, Evans JEE, Sawaya MRR, Cascio D, Eisenberg DSS, Gonen T and Rodriguez JAA, Nat. Struct. Mol. Biol, 2018, 25, 131–134. [PubMed: 29335561]
13. van Genderen E, Clabbers MTB, Das PP, Stewart A, Nederlof I, Barentsen KC, Portillo Q, Pannu NS, Nicolopoulos S, Gruene T and Abrahams JP, Acta Crystallogr. Sect. A, 2016, 72, 236–242.
14. Jones CG, Martynowycz MW, Hattne J, Fulton TJ, Stoltz BM, Rodriguez JA, Nelson HM and Gonen T, ACS Cent. Sci, 2018, 4, 1587–1592. [PubMed: 30555912]
15. Henderson R, Q. Rev. Biophys, 1995, 28, 171–193. [PubMed: 7568675]
16. Shi D, Lewis MRR, Young HSS and Stokes DLL, J. Mol. Biol, 1998, 284, 1547–1564. [PubMed: 9878370]
17. Jiang J, Jorda JLL, Yu J, Baumes LAA, Mugnaioli E, Diaz-Cabanas MJJ, Kolb U and Corma A, Science, 2011, 333, 1131–1134. [PubMed: 21868673]
18. Kühlbrandt W, Science, 2014, 343, 1443–1444. [PubMed: 24675944]
19. Henderson R, Angew. Chemie Int. Ed, 2018, 57, 10804–10825.
20. Gorelik TE, Stewart AA and Kolb U, J. Microsc, 2011, 244, 325–331. [PubMed: 21992494]
21. Su J, Kapaca E, Liu L, Georgieva V, Wan W, Sun J, Valtchev V, Hovmöller S and Zou X, Micropor. Mesopor. Mat, 2014, 189, 115–125.
22. Nannenga BL, Shi D, Leslie AGW and Gonen T, Nat. Methods, 2014, 11, 927–930. [PubMed: 25086503]
23. De La Cruz MJ, Hattne J, Shi D, Seidler P, Rodriguez J, Reyes FE, Sawaya MR, Cascio D, Weiss SC, Kim SK, Hinck CS, Hinck AP, Calero G, Eisenberg D and Gonen T, Nat. Methods, 2017, 14, 399–402. [PubMed: 28192420]

24. Xu H, Lebrette H, Clabbers MTB, Zhao J, Griese JJ, Zou X and Högbom M, Sci. Adv, 2019, 5, DOI: 10.1126/sciadv.aax4621.
25. Liu S and Gonen T, Commun. Biol, 2018, 1, 1–6. [PubMed: 29809203]
26. Purdy MD, Shi D, Chrustowicz J, Hattne J, Gonen T and Yeager M, Proc. Natl. Acad. Sci, 2018, 115, 13258–13263. [PubMed: 30530702]
27. Clabbers MTB, Fisher SZ, Coinçon M, Zou X and Xu H, Commun. Biol, 2020, 3, DOI: 2020.04.27.064188.
28. Martynowycz MW and Gonen T, bioRxiv, 2020, DOI: 2020.05.25.115246.
29. Vergara S, Lukes DA, Martynowycz MW, Santiago U, Plascencia-Villa G, Weiss SC, De La Cruz MJ, Black DM, Alvarez MM, López-Lozano X, Barnes CO, Lin G, Weissker GC, Whetten RL, Gonen T, Yacaman MJ and Calero G, J. Phys. Chem. Lett, 2017, 8, 5523–5530. [PubMed: 29072840]
30. Nannenga BL, Struct. Dyn, 2020, 7, DOI: 10.1063/1.5128226.
31. Levine AM, Bu G, Biswas S, Tsai EHR, Braunschweig AB and Nannenga BL, Chem. Commun, 2020, 56, 4204–4207.
32. Dick M, Sarai NS, Martynowycz MW, Gonen T and Arnold FH, J. Am. Chem. Soc, 2019, 141, 19817–19822. [PubMed: 31747522]
33. Clabbers MTB, Gruenevan T, Genderen E and Abrahams JP, Acta Cryst. A, 2019, 75, 82–93.
34. Jones CG, Asay M, Kim LJ, Kleinsasser JF, Saha A, Fulton TJ, Berkley KR, Cascio D, Malyutin AG, Conley MP, Stoltz BM, Lavallo V, Rodríguez JA and Nelson HM, ACS Cent. Sci, 2018, 4, 1587–1592. [PubMed: 30555912]
35. Zhou H, Luo F, Luo Z, Li D, Liu C and Li X, Anal. Chem, 2019, 91, 10996–11003. [PubMed: 31334636]
36. Hamada H, Nakamuro T, Yamashita K, Yanagisawa H, Nureki O, Kikkawa M, Harano K, Shang R and Nakamura E, Bull. Chem. Soc. Jpn, 2020, 93, 776–782.
37. Wang Y, Yang T, Xu H, Zou X and Wan W, J. Appl. Crystallogr, 2018, 51, 1094–1101.
38. Curtis BJ, Kim LJ, Wrobel CJJ, Eagan JM, Smith RA, Burch JE, Le HH, Artyukhin AB, Nelson HM and Schroeder FC, Org. Lett, 2020, DOI: 10.1021/acs.orglett.0c02038.
39. Luft JRR, Wolfley JRR and Snell EHH, Cryst. Growth Des, 2011, 11, 651–663.
40. Gonen T, in Electron Crystallography of Soluble and Membrane Proteins: Methods and Protocols, eds. Schmidt-Krey I and Cheng Y, Humana Press, Totowa, NJ, 2013, pp. 153–169.
41. Dörner K, Martin-Garcia JM, Kupitz C, Gong Z, Mallet TC, Chen L, Wachter RM and Fromme P, Cryst. Growth Des, 2016, 16, 3838–3845.
42. Shi D, Nannenga BL, De La Cruz MJ, Liu J, Sawtelle S, Calero G, Reyes FE, Hattne J and Gonen T, Nat. Protoc, 2016, 11, 895–904. [PubMed: 27077331]
43. Parker JL and Newstead S, Adv. Exp. Med. Biol, 2016, 922, 61–72. [PubMed: 27553235]
44. Gruene T, Wennmacher JTC, Zaubitzer C, Holstein JJ, Heidler J, Fecteau-Lefebvre A, De Carlo S, Müller E, Goldie KN, Regeni I, Li T, Santiso-Quinones G, Steinfeld G, Handschin S, van Genderen E, van Bokhoven JA, Clever GH and Pantelic R, Angew. Chem.Int. Ed, 2018, 57, 16313–16317.
45. Hattne J, Shi D, Glynn C, Te Zee C, Gallagher-Jones M, Martynowycz MW, Rodriguez JA and Gonen T, Structure, 2018, 26, 759–766. [PubMed: 29706530]
46. Kabsch W, Acta Crystallogr. Sect. D Struct. Biol, 2010, 66, 125–132.
47. Battye TGG, Kontogiannis L, Johnson O, Powell HR and Leslie AGW, Acta Crystallogr. Sect. D Struct. Biol, 2011, 67, 271–281.
48. Leslie AGW and Powell HR, in Evolving Methods for Macromolecular Crystallography, eds. Read RJ and Sussman JL, Springer Netherlands, Dordrecht, 2007, pp. 41–51.
49. Sheldrick GM, Acta Crystallogr. Sect. D Struct. Biol, 2010, 66, 479–485.
50. Rodriguez JAA, Ivanova MII, Sawaya MRR, Cascio D, Reyes FEE, Shi D, Sangwan S, Guenther ELL, Johnson LMM, Zhang M, Jiang L, Arbing MAA, Nannenga BLL, Hattne J, Whitelegge J, Brewster ASS, Messerschmidt M, Boutet SS, Sauter NKK, Gonen T and Eisenberg DSS, Nature, 2015, 525, 486–490. [PubMed: 26352473]

51. Andrusenko I, Hamilton V, Mugnaioli E, Lanza A, Hall C, Potticary J, Hall SR and Gemmi M, Angew. Chemie Int. Ed, 2019, 58, 10919–10922.
52. Seidler PM, Boyer DR, Rodriguez JA, Sawaya MR, Cascio D, Murray K, Gonen T and Eisenberg DS, Nat. Chem, 2018, 10, 170–176. [PubMed: 29359764]
53. Krotee P, Griner SL, Sawaya MR, Cascio D, Rodriguez JA, Shi D, Philipp S, Murray K, Saelices L, Lee J, Seidler P, Glabe CG, Jiang L, Gonen T and Eisenberg DS, J. Biol. Chem, 2018, 293, 2888–2902. [PubMed: 29282295]
54. Morris RJ and Bricogne G, Acta Crystallogr. Sect. D Struct. Biol, 2003, 59, 615–617.
55. Sawaya MRR, Rodriguez J, Cascio D, Collazo MJJ, Shi D, Reyes FEE, Hattne J, Gonen T and Eisenberg DSS, Proc. Natl. Acad. Sci, 2016, 113, 11232–11236. [PubMed: 27647903]
56. Krotee P, Rodriguez JA, Sawaya MR, Cascio D, Reyes FE, Shi D, Hattne J, Nannenga BL, Oskarsson ME, Philipp S, Griner S, Jiang L, Glabe CG, Westermark GT, Gonen T and Eisenberg DS, Elife, 2017, DOI: 10.7554/elife.19273.
57. Westermark P, Wernstedt C, Wilander E, Hayden DWW, O'Brien TD and Johnson KHH, Proc. Natl. Acad. Sci, 1987, 84, 3881–3885. [PubMed: 3035556]
58. Cooper GJJS, Leighton B, Dimitriadis GDD, Parry-Billings M, Kowalchuk JMM, Howland K, Rothbard JBB, Willis ACC and Reid KBBM, Proc. Natl. Acad. Sci, 1988, 85, 7763–7766. [PubMed: 3051005]
59. Fernández MSS, Cell Calcium, 2014, 56, 416–427. [PubMed: 25224501]
60. Luca S, Yau W-M, Leapman R and Tycko R, Biochemistry, 2007, 46, 13505–13522. [PubMed: 17979302]
61. Liu C, Zhao M, Jiang L, Cheng PN, Park J, Sawaya MR, Pensalfini A, Gou D, Berk AJ, Glabe CG, Nowick J and Eisenberg D, Proc. Natl. Acad. Sci, 2012, 109, 20913–20918. [PubMed: 23213214]
62. Foos N, Seuring C, Schubert R, Burkhardt A, Svensson O, Meents A, Chapman HNN and Nanao MHH, Acta Crystallogr. Sect. D Struct. Biol, 2018, 74, 366–378. [PubMed: 29652263]
63. Vargesson N, Birth Defects Res. C Embryo Today, 2015, 105, 140–156. [PubMed: 26043938]
64. Galea AM and Murray V, Cancer Inform, 2008, 6, 315–355. [PubMed: 19259415]
65. Parsons S, Tetrahedron: Asymmetry, 2017, 28, 1304–1313.
66. Wenzel TJ, Tetrahedron: Asymmetry, 2017, 28, 1212–1219.
67. Batista ANL, dos Santos FM Jr, Batista JM and Cass QB, Molecules, 2018, 23, 492.
68. Brázda P, Palatinus L and Babor M, Science, 2019, 364, 667–669. [PubMed: 31097664]
69. Bode HB and Müller R, Angew. Chem. Int. Ed, 2005, 44, 6828–6846.
70. Velásquez JE and Van der Donk WA, Curr. Opin. Chem. Biol, 2011, 15, 11–21. [PubMed: 21095156]
71. Shen B, Cell, 2015, 163, 1297–1300. [PubMed: 26638061]
72. Rutledge PJ and Challis GL, Nat. Rev. Microbiol, 2015, 13, 509–523. [PubMed: 26119570]
73. Katz L and Baltz RH, J. Ind. Microbiol. Biotechnol, 2016, 43, 155–176. [PubMed: 26739136]
74. Ziemert N, Alanjary M and Weber T, Nat. Prod. Rep, 2016, 33, 988–1005. [PubMed: 27272205]
75. Tracanna V, de Jong A, Medema MH and Kuipers OP, FEMS Microbiol. Rev, 2017, 41, 417–429. [PubMed: 28402441]
76. Medema MH and Fischbach MA, Nat. Chem. Biol, 2015, 11, 639–648. [PubMed: 26284671]
77. Ren H, Hu P and Zhao H, Biotechnol. Bioeng, 2017, 114, 1847–1854. [PubMed: 28401530]
78. Choi SS, Katsuyama Y, Bai L, Deng Z, Ohnishi Y and Kim ES, Curr. Opin. Microbiol, 2018, 45, 53–60. [PubMed: 29510374]
79. Huo L, Hug JJ, Fu C, Bian X, Zhang Y and Müller R, Nat. Prod. Rep, 2019, 36, 1412–1436. [PubMed: 30620035]
80. Li L, Liu X, Jiang W and Lu Y, Front. Microbiol, 2019, DOI : 10.3389/fmicb.2019.02467.
81. Palazzotto E, Tong Y, Lee SY and Weber T, Biotechnol. Adv, 2019, 37, 107366. [PubMed: 30853630]
82. Zhang JJ, Yamanaka K, Tang X and Moore BS, Method. Enzymol, 2019, 621, 87–110.
83. Oikawa H, Biosci. Biotechnol. Biochem, 2020, 84, 433–444. [PubMed: 31738699]

84. Traxler MF and Kolter R, Nat. Prod. Rep, 2015, 32, 956–970. [PubMed: 26000872]
85. Zarins-Tutt JS, Barberi TT, Gao H, Mearns-Spragg A, Zhang L, Newman DJ and Goss RJM, Nat. Prod. Rep, 2016, 33, 54–72. [PubMed: 26538321]
86. Molloy EM and Hertweck C, Curr. Opin. Microbiol, 2017, 39, 121–127. [PubMed: 29169087]
87. Mao D, Okada BK, Wu Y, Xu F and Seyedsayamdost MR, Curr. Opin. Microbiol, 2018, 45, 156–163. [PubMed: 29883774]
88. Doroghazi JR, Albright JC, Goering AW, Ju KS, Haines RR, Tchalukov KA, Labeda DP, Kelleher NL and Metcalf WW, Nat. Chem. Biol, 2014, 10, 963–968. [PubMed: 25262415]
89. Kersten RD, Yang YL, Xu Y, Cimermancic P, Nam SJ, Fenical W, Fischbach MA, Moore BS and Dorrestein PC, Nat. Chem. Biol, 2011, 7, 794–802. [PubMed: 21983601]
90. Covington BC, McLean JA and Bachmann BO, Nat. Prod. Rep, 2017, 34, 6–24. [PubMed: 27604382]
91. Breton RC and Reynolds WF, Nat. Prod. Rep, 2013, 30, 501–524. [PubMed: 23291908]
92. Robinette SL, Brüschweiler R, Schroeder FC and Edison AS, Acc. Chem. Res, 2012, 45, 2, 288–297. [PubMed: 21888316]
93. Bouslimani A, Sanchez LM, Garg N and Dorrestein PC, Nat. Prod. Rep, 2014, 31, 718–729. [PubMed: 24801551]
94. Jansma A, Chuan T, Albrecht RW, Olson DL, Peck TL and Geierstanger BH, Anal. Chem, 2005, 77, 6509–6515. [PubMed: 16194121]
95. Gronquist M, Meinwald J, Eisner T and Schroeder FC, J. Am. Chem. Soc, 2005, 127, 10810–10811. [PubMed: 16076169]
96. Schroeder FC and Gronquist M, Angew. Chem Int. Ed, 2006, 45, 7122–7131.
97. Schroeder FC, Taggi AE, Gronquist M, Malik RU, Grant JB, Eisner T and Meinwald J, Proc. Natl. Acad. Sci, 2008, 105, 14283–14287. [PubMed: 18794518]
98. Olson DL, Norcross JA, O'Neil-Johnson M, Molitor PF, Detlefsen DJ, Wilson AG and Peck TL, Anal. Chem, 2004, 76, 2966–2974. [PubMed: 15144211]
99. Inokuma Y, Yoshioka S, Ariyoshi J, Arai T, Hitora Y, Takada K, Matsunaga S, Rissanen K and Fujita M, Nature, 2013, 495, 461–466. [PubMed: 23538828]
100. Mori K, Akasaka K and Matsunaga S, Tetrahedron, 2014, 70, 392–401.
101. Ramadhar TR, Zheng SL, Chen YS and Clardy J, Acta Crystallogr. Sect. A Found. Crystallogr, 2015, 71, 46–58.
102. Inokuma Y, Ukegawa T, Hoshino M and Fujita M, Chem. Sci, 2016, 7, 3910–3913. [PubMed: 30155035]
103. Lee S, Kapustin EA and Yaghi OM, Science, 2016, 353, 808–811. [PubMed: 27540171]
104. Morishita Y, Sonohara T, Taniguchi T, Adachi K, Fujita M and Asai T, Org. Biomol. Chem, 2020, 18, 2813–2816. [PubMed: 32219266]
105. Kersten RD, Lee S, Fujita D, Pluskal T, Kram S, Smith JE, Iwai T, Noel JP, Fujita M and Weng JK, J. Am. Chem. Soc, 2017, 139, 16838–16844. [PubMed: 29083151]
106. Brkljaca R, Schneider B, Hidalgo W, Otálvaro F, Ospina F, Lee S, Hoshino M, Fujita M and Urban S, Molecules, 2017, 22, 211.

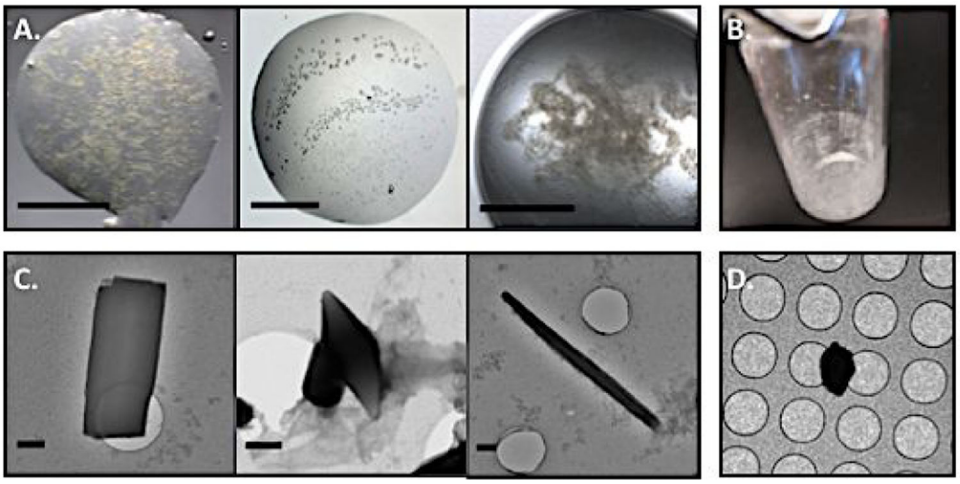

Figure 1.

Examples of crystals used for MicroED. A. Crystal drops in an optical microscope; the size bar is 500 μm. B. Amorphous powder from flash chromatography which can be directly applied to a grid for MicroED. C. Examples of nanocrystals identified by negative stain, size bar is 400 nm. D. Nanocrystals were identified on a cryo-EM grid in the TEM.

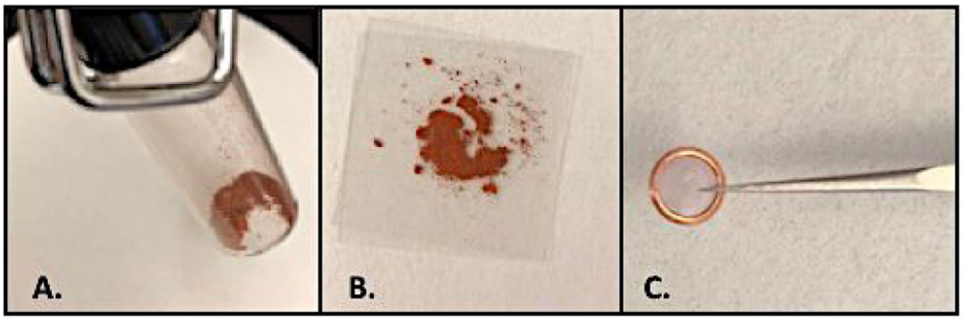

Figure 2.

Grid preparation for MicroED. An amorphous powder sample (A) is homogenized between glass cover slides (B) and deposited on a holey carbon quantifoil grid (C) for examination in the TEM.

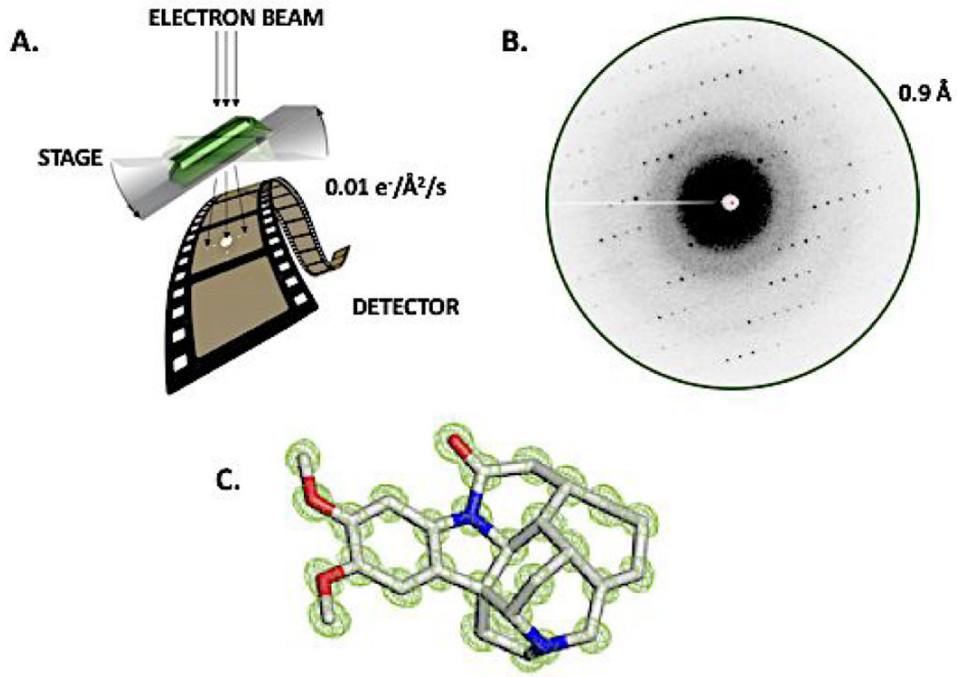

Figure 3.

Continuous rotation MicroED data collection and processing. A. The sample is continuously rotated during data collection and data collected on a fast camera as a movie. B. Each frame in the movie is a diffraction pattern representing a wedge in reciprocal space. C. The atomic resolution structure of brucine at 0.9 Å resolution was determined by MicroED from femtogram amounts of material 14.

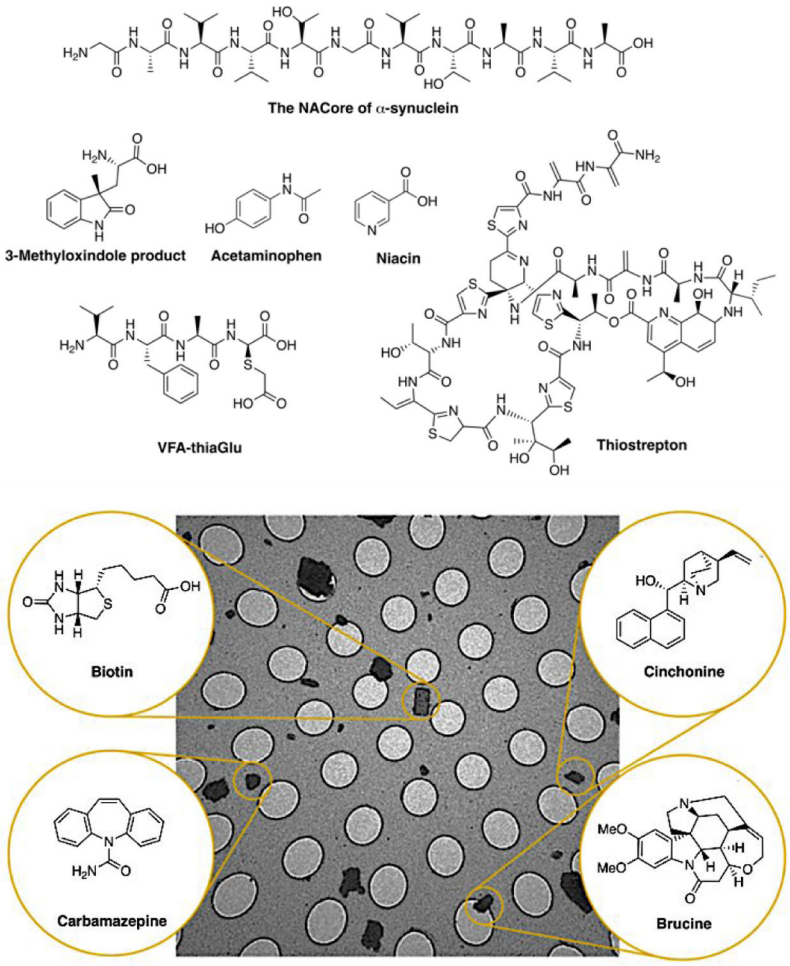

Figure 4.

Selection of structures of natural products and derivatives determined by MicroED. The structures of brucine, biotin, carbamazepine, and cinchonine were determined from a mixture of the four compounds.

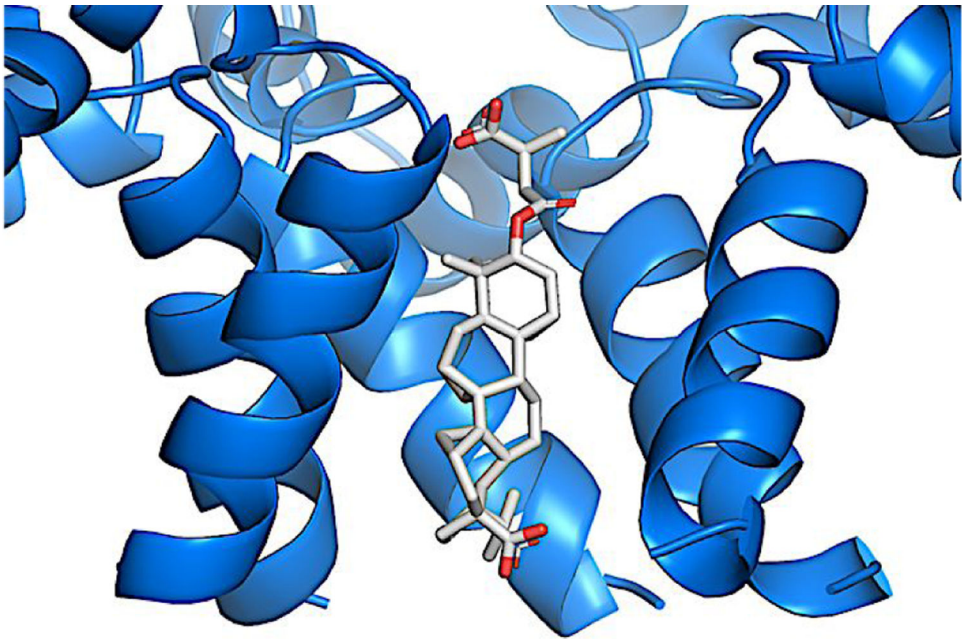

Figure 5.
The structure of bevirimat bound to its target HIV-1 Gag was the first example in MicroED where a protein was co crystallized with a ligand.

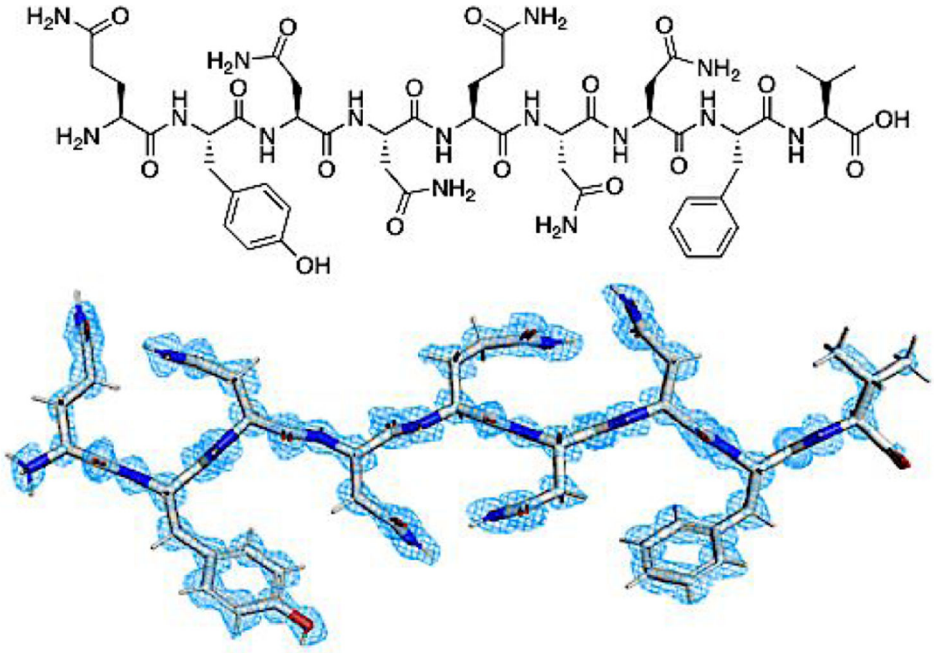

Figure 6.

Sub-ångström resolution MicroED structure of prion proto-PrPSc determined from nanocrystals diffracting to 0.72 Å. Merging diffraction from multiple crystals gave a 0.75-Å-resolution dataset with high completeness from which the structure was solved ab initio. The structure shows features that are invisible in the X-ray structure, such as unambiguously assigned hydrogens.

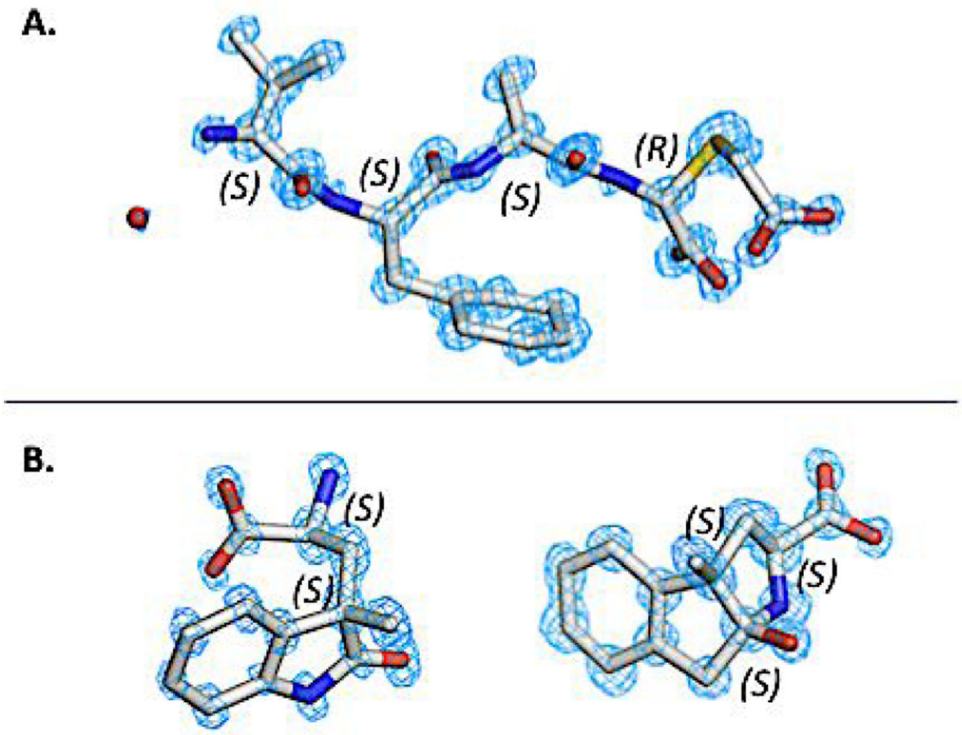

Figure 7.
Examples of determining stereochemistry in MicroED. A. 0.9-Å resolution structure of VFA-thiaGlu. B. 0.9 Å structures of 3-methyloxindole (left) and 1-methyl-2-indanone (right) containing amino acids.